Vertically Oriented 1D Capping Layer Enabled by Bilayer Interface Engineering for Efficient and Stable Inverted Perovskite Solar Cells

Hongyu Chen[1,2#], Xueliang Zhu[1#]*, Kangwei Mo[4#], Ning Ma[1], Bianyuan Ren[1], Xinyu Jiang[1], Man Yang[3], Yibo Tu[2], Guodong Li[2], Wensheng Yan[2]*, Gongxun Bai[1]*

[1]College of Science, China Jiliang University, Hangzhou 310018, China.

[2]Institute of Carbon Neutrality and New Energy, School of Electronics and Information Engineering, Hangzhou Dianzi University, Hangzhou 310018, China.

[3]College of Physics and Electronic Science, Hubei Normal University, Huangshi, 435002, China.

[4]School of Physics and Technology, Wuhan University, Wuhan 430072, China.

[#]These authors contribute equally to this work.

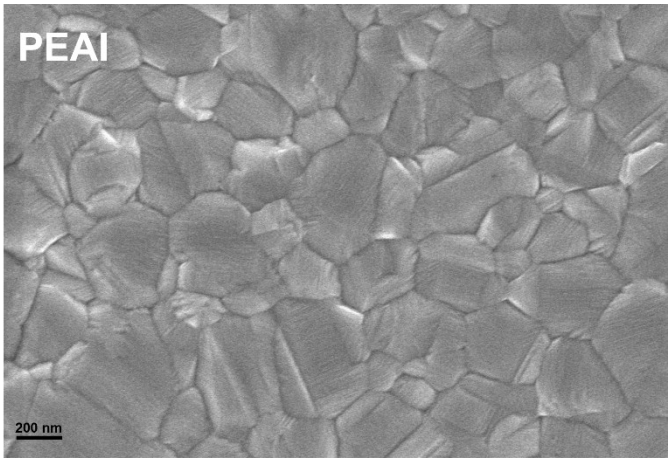

Figure S1. Top-view SEM images of PEAI-treated perovskite film.

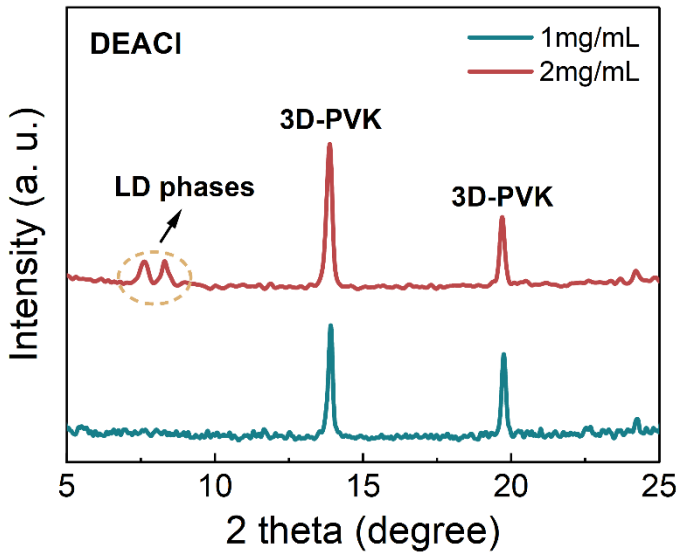

Figure S2. XRD spectra of DEACl-treated samples at different concentrations.

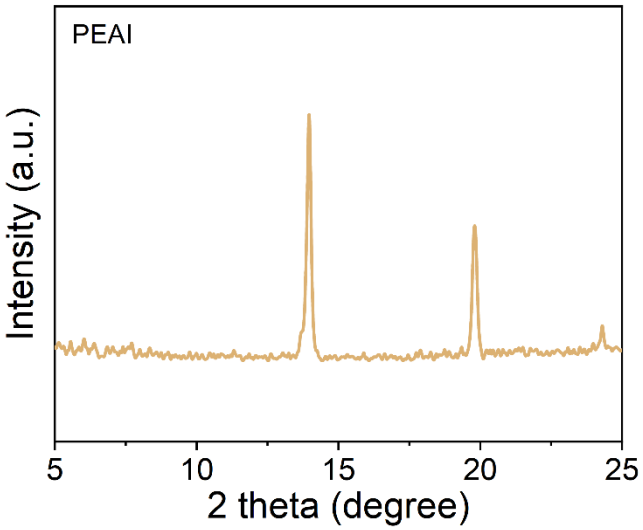

Figure S3. XRD spectra of PEAI-treated samples.

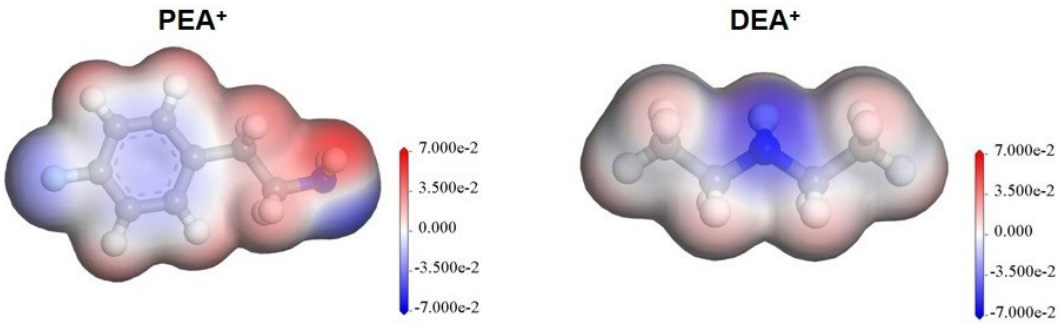

Figure S4. The ESP distributions of PEA and DEA.

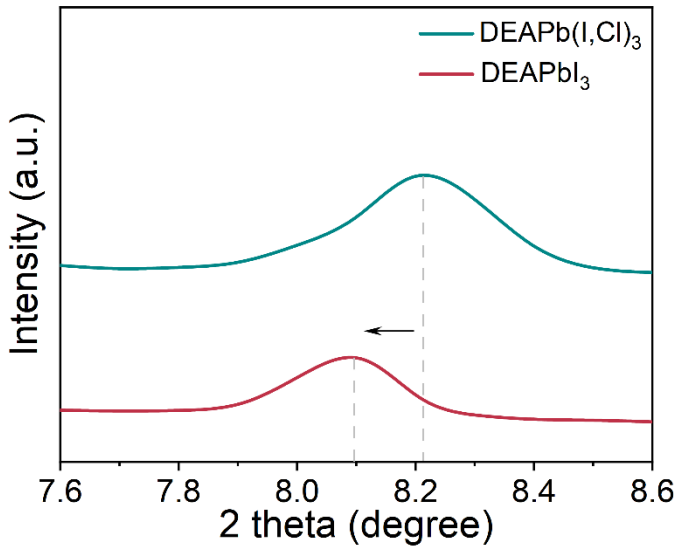

Figure S5. XRD spectra of DEAPb(I, Cl)$_3$ and DEAPbI$_3$ films.

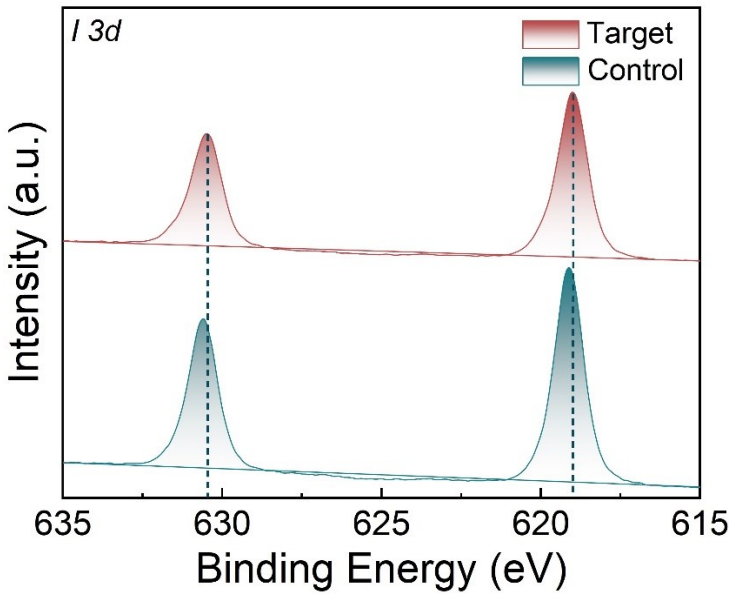

Figure S6. XPS spectra of I 3d for control and target films.

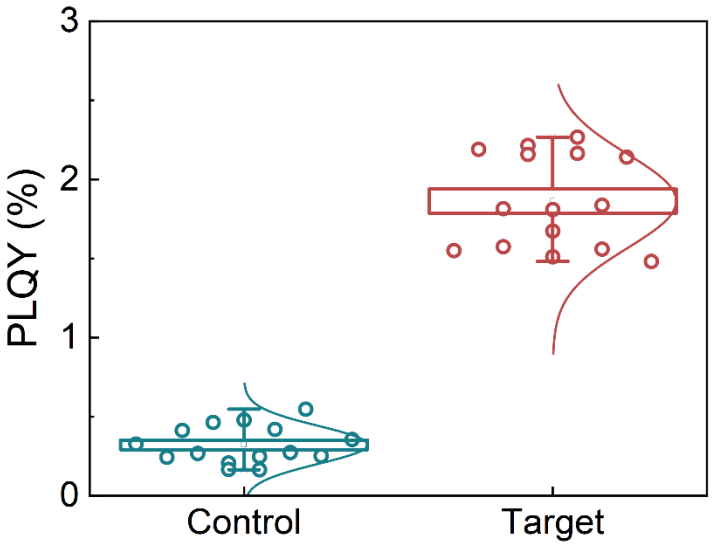

Figure S7. PLQY distribution of control and target films.

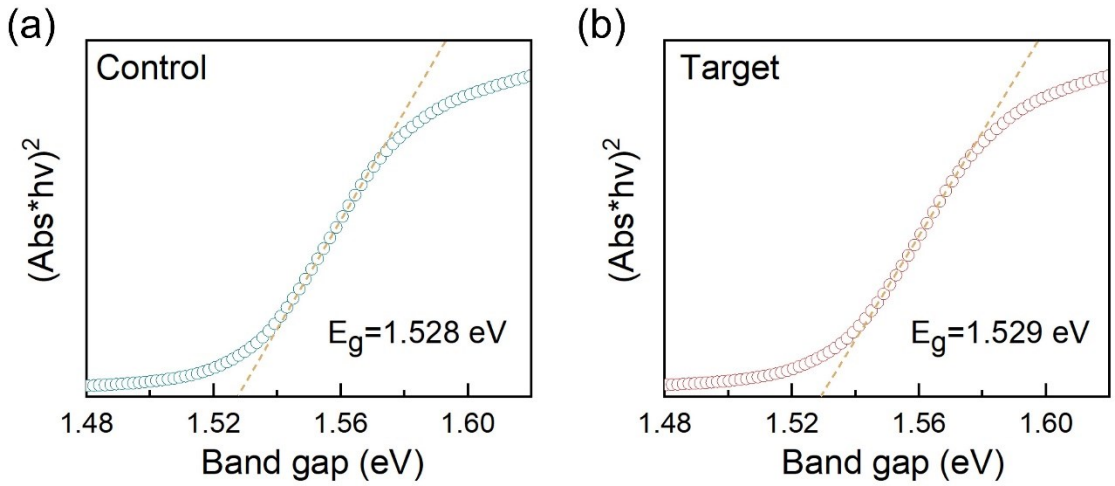

Figure S8. The Tauc plots of the (a) control and (b) target perovskite films.

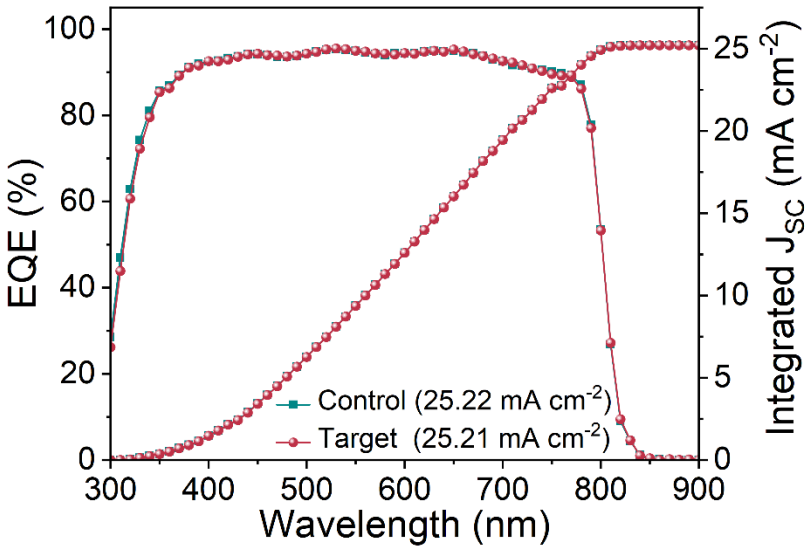

Figure S9. The EQE spectra perovskite devices. The integrated current density and the scanned J_{SC} are within 5% difference which is within the accuracy confidence of the measurements.

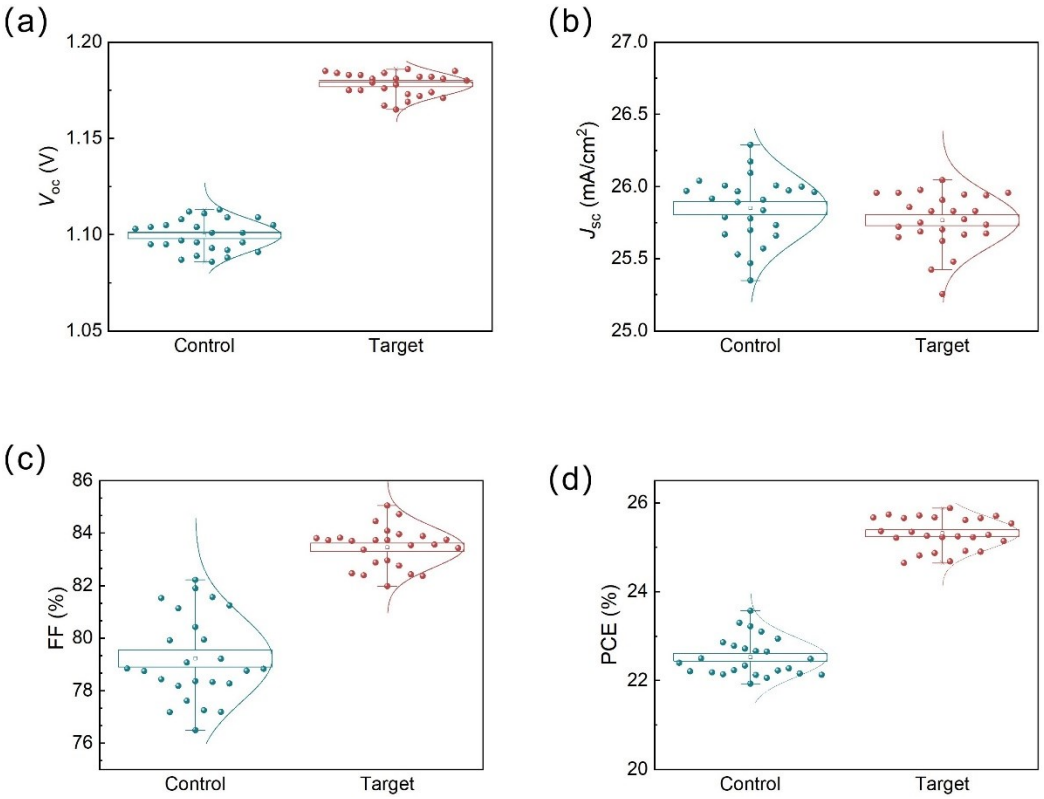

Figure S10. Statistics of (a) V_{OC}, (b) J_{SC}, (c) FF and (d) PCE of the control and target devices.

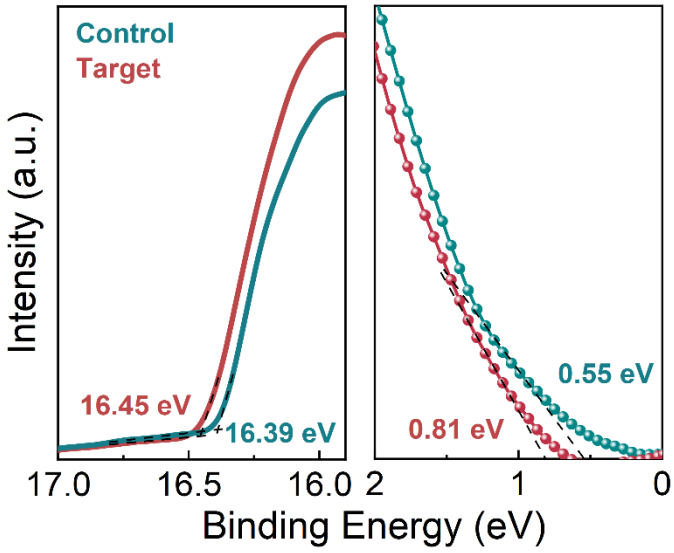

Figure S11. The UPS spectra of control and target films.

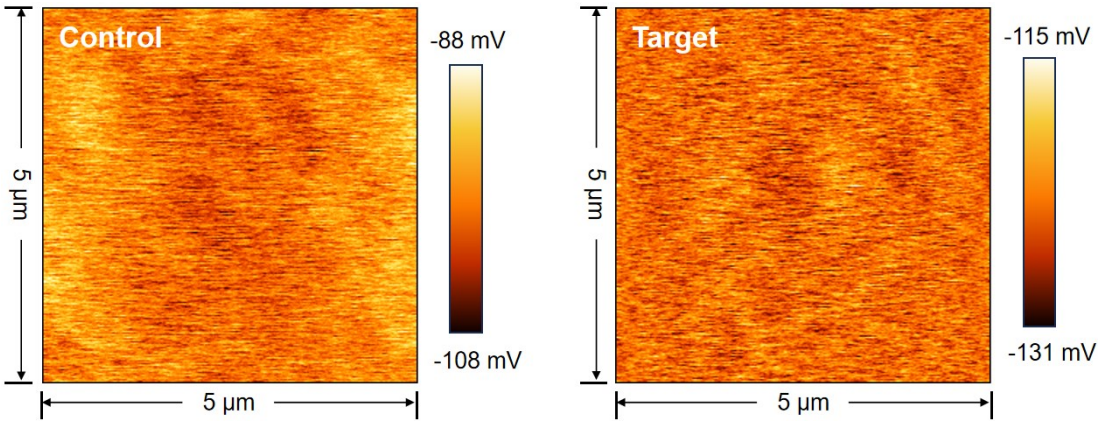

Figure S12. The potential images from KPFM of control and target films.

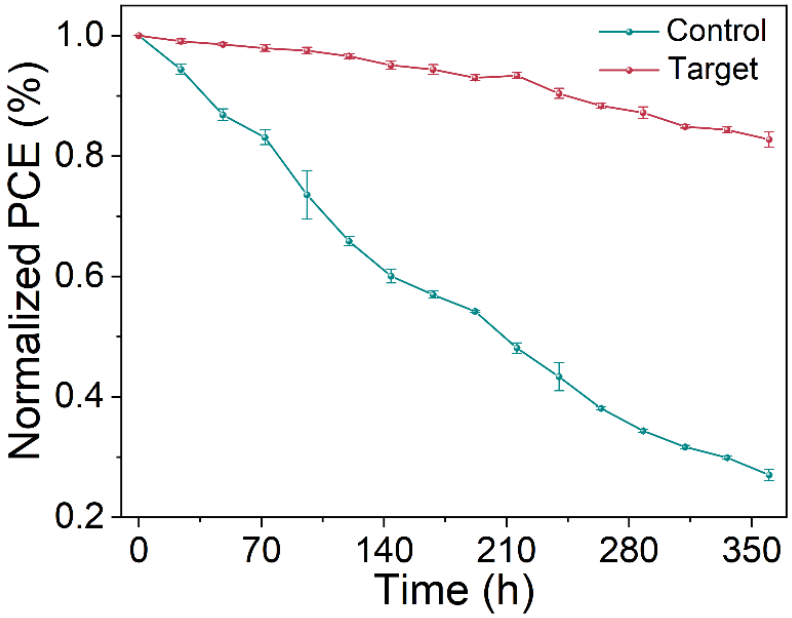

Figure S13. Efficiency statistics of unencapsulated devices under continuous illumination of one sun in air.

Table S1. Summary of the photovoltaic parameters of the PSCs devices. SC and FB stand for short circuit and forward bias, respectively.

Devices	**Scan direction**	J_{SC} **(mA/cm^2)**	V_{OC} **(V)**	**FF (%)**	**PCE (%)**
Control devices					
Champion	SC-FB	26.0	1.11	79.5	22.9
	FB-SC	26.0	1.11	81.9	23.6
Target devices					
Champion	SC-FB	26.0	1.18	82.4	25.3
	FB-SC	26.0	1.18	84.5	25.9

Table S2. Photovoltaic parameters of PSCs based on 1D perovskites, comparing recent literature and this work.

1D perovskite	Device structure	PCE (%)	Year	Ref.
$BnPbI_3$	ITO/PTAA/PVK/C_{60}/BCP/Ag	21.17	2021	[1]
Me_3SPbI_3	ITO/SnO_2/PVSK/spiro-OMeTAD/Ag	22.07	2021	[2]
$FA(CBA)PbI_4$	ITO/SnO_2/PVSK/spiro-OMeTAD/MoO_3/Ag	21.95	2021	[3]
$EMIMPbI_3$	FTO/c-TiO_2/SnO_2/PVSK/spiro-OMeTAD/Ag	22.14	2021	[4]
$DEAECPbI_3$	ITO/SnO_2/PVSK/spiro-OMeTAD/Ag	22.90	2021	[5]
$TMIMPbI_3$	ITO/SnO_2/PVSK/spiro-OMeTAD/Au	22.70	2021	[6]
$TPPbI_3$	ITO/PTAA/PVK/C_{60}/BCP/Ag	22.00	2022	[7]
(m-PBA) Pb_2I_6	ITO/SnO_2/PVSK/spiro-OMeTAD/Au	23.84	2022	[8]
$PbI_2(Phen)$	ITO/SnO_2/PVSK/spiro-OMeTAD/Ag	23.30	2022	[9]
$(C6)_2PbI_4$	FTO/c-TiO_2/PVSK/spiro-OMeTAD/Au	23.11	2022	[10]
$iprPbI_3$	FTO/SnO_2/PVSK/spiro-OMeTAD/Au	24.43	2022	[11]
$ABTPbI_3$	ITO/MeO-2PACz/Perovskite/C_{60}/BCP/Cu	23.27	2023	[12]
F-$iprPbI_3$	FTO/SnO_2/PVSK/spiro-OMeTAD/Au	24.05	2023	[13]
$CPMIMPbI_3$	ITO/SnO_2/PVSK/spiro-OMeTAD/Au	24.13	2023	[14]
$TAPbI_3$	ITO/SnO_2/PVSK/spiro-OMeTAD/Au	23.87	2023	[15]
$TEAPbI_3$	FTO/c-TiO_2/SnO_2/PVSK/spiro-OMeTAD/Au	24.41	2023	[16]
$PFAPbI_2Cl$	FTO/SnO_2/PVSK/spiro-OMeTAD/Au	24.90	2023	[17]
$TBMAPbI_3$	FTO/c-TiO_2/SnO_2/PVK/spiro-OMeTAD/Ag	25.09	2023	[18]
$ChPbI_3$	ITO/MeO-2PACz: Me-4PACz/PVK/$PC_{61}BM$/BCP/Ag	24.03	2024	[19]

$TZCPbI_3$	ITO/NiO_X/Me-4PACz/PVK /PCBM/BCP/Ag	25.28	2024	[20]
$(MTIm)PbI_3$	ITO/MeO-2PACz/PVK/$PC_{61}BM$/BCP/Ag	23.80	2024	[21]
$MDAPb_2I_6$	ITO/PTAA/PVK/ C_{60}/ BCP/ Cu	23.80	2024	[22]
$EMIMPbI_3$	ITO/SnO_2/PVSK/spiro-OMeTAD/Au	24.75	2024	[23]
$SMORPbI_3$	ITO/SAM/ PVK /C_{60}/BCP/Ag	25.60	2025	[24]
$PYFPbI_3$	ITO/MeO-2PACz/PVK/C_{60}/BCP/Ag	25.39	2025	[25]
$M\text{-}NMAPbI_3$	FTO/SnO_2/PVSK/spiro-OMeTAD/Au	25.51	2025	[26]
$(QA)PbI_4$	ITO/SnO_2/PVK/spiro-OMeTAD/Au	24.80	2025	[27]
TESI-PbI_2	ITO/SnO_2/PVK/spiro-OMeTAD/Ag	25.03	2025	[28]
$DEAPbI_3$	FTO/NiO_X/SAMs/PVK/C_{60}/BCP/Cu	25.90	2025	This work

1. Zhan Y. *et al.* Elastic Lattice and Excess Charge Carrier Manipulation in 1D-3D Perovskite Solar Cells for Exceptionally Long-Term Operational Stability. *Adv Mater* **33**, 2105170 (2021).
2. Ge C. *et al.* Mixed Dimensional Perovskites Heterostructure for Highly Efficient and Stable Perovskite Solar Cells. *Solar RRL* **6**, 2100879 (2021).
3. Wang J. *et al.* Growth of 1D Nanorod Perovskite for Surface Passivation in $FAPbI_3$ Perovskite Solar Cells. *Small* **18**, 2104100 (2022).
4. Wei N. *et al.* Multi-Level Passivation of $MAPbI_3$ Perovskite for Efficient and Stable Photovoltaics. *Adv. Func. Mater.* **32**, 2108944 (2021).
5. Kong T. *et al.* Perovskitoid-Templated Formation of a 1D@3D Perovskite Structure toward Highly Efficient and Stable Perovskite Solar Cells. *Adv. Energy Mater.* **11**, 2101018 (2021).
6. Zhang H. *et al.* Highly Efficient 1D/3D Ferroelectric Perovskite Solar Cell. *Adv. Func. Mater.* **31**, 2100205 (2021).
7. Jiao H. *et al.* Perovskite grain wrapping by converting interfaces and grain boundaries into robust and water-insoluble low-dimensional perovskites. *Sci. Adv.* **8**, eabg4524 (2022).
8. Chen J. *et al.* Highly efficient and stable perovskite solar cells enabled by low-dimensional perovskitoids. *Sci. Adv.* **8**, 9 (2022).
9. Chen Q. *et al.* Stable one dimensional (1D)/three dimensional (3D) perovskite solar cell with an efficiency exceeding 23%. *InfoMat* **4**, (2022).
10. Hu Y. *et al.* Amino Acid-Based Low-Dimensional Management for Enhanced Perovskite Solar Cells. *Solar RRL* **6**, 2200168 (2022).
11. Chen R. *et al.* Conformal Imidazolium 1D Perovskite Capping Layer Stabilized 3D Perovskite Films for Efficient Solar Modules. *Adv. Sci.* **9**, 2204017 (2022).
12. Wang D. *et al.* Binary Microcrystal Additives Enabled Antisolvent-Free Perovskite Solar Cells with High Efficiency and Stability. *Adv. Energy Mater.* **13**, 2203649 (2022).
13. Chen R. *et al.* Patch-healed grain boundary strategy to stabilize perovskite films for high-performance solar modules. *Nano Energy* **115**, 108759 (2023).
14. Wang F. *et al.* Ionic liquid engineering enabled in-plane orientated 1D perovskite nanorods for efficient mixed-dimensional perovskite photovoltaics. *Infomat* **5**, e12459 (2023).
15. Chen Z. *et al.* Perovskite Grain-Boundary Manipulation Using Room-Temperature Dynamic Self-Healing "Ligaments" for Developing Highly Stable Flexible Perovskite

Solar Cells with 23.8% Efficiency. *Adv. Mater.* **35**, 2300513 (2023).
16. Wei N. *et al.* Post-Treatment-Free Dual-Interface Passivation via Facile 1D/3D Perovskite Heterojunction Construction. *J. Am. Chem. Soc.* **3**, 3324-3332 (2023).
17. Ye F. *et al.* Tailoring Low-Dimensional Perovskites Passivation for Efficient Two-Step-Processed $FAPbI_3$ Solar Cells and Modules. *Adv. Energy Mater.* **14**, 2302775 (2023).
18. Miao Y. *et al.* Green solvent enabled scalable processing of perovskite solar cells with high efficiency. *Nat. Sustain.* **6**, 1465-1473 (2023).
19. Ji R. *et al.* Spontaneous Formation of 1D/3D Perovskite Heterojunctions for Efficient Inverted Perovskite Solar Cells. *Adv. Energy Mater.* **14**, 2304126 (2024).
20. Zhou X. *et al.* N-Type Doping Characteristics Enabled by 1D Perovskite for Advancing Perovskite Photovoltaics: From 1.55 to 1.85 eV Bandgap. *Adv. Energy Mater.* **15**, 2501553 (2025).
21. Zhou C. *et al.* Dual interfacial modification with 1D perovskite for self-assembled monolayer based inverted perovskite solar cells. *Nano Energy* **128**, 109811 (2024).
22. Jiang C. *et al.* In-Situ Growth of One-Dimensional Blocking Layer to Mitigate Deficient Surface of Single-Crystal Perovskites. *Angew. Chem. Int. Ed. Engl.* **63**, e202412485 (2024).
23. Wang F. *et al.* Ionic Liquid-Induced 1D Perovskite: Exploring 1D Perovskite Structure to 1D/3D Heterojunction-Based Photovoltaics. *Adv. Energy Mater.* **14**, 2100021 (2024).
24. Li S. *et al.* Anion-Cation Synergistic Regulation of Low-Dimensional Perovskite Passivation Layer for Perovskite Solar Cells. *Adv. Mater*. **37**, 2500988 (2025).
25. Liu N. *et al.* Chemical Bond Management of FA-Based Mixed Halide Perovskites for Stable and High-Efficiency Solar Cells. *Adv. Energy Mater.* **15**, 2405212 (2025).
26. Liang L. *et al.* Formation Dynamics of Thermally Stable 1D/3D Perovskite Interfaces for High-Performance Photovoltaics. *Adv. Mater.* **37**, 2413841 (2025).
27. Tang Y. *et al.* High-Performance Perovskite Solar Cells Enabled by One-Dimensional Capping Layer with Conjugated Ligands. *ACS Appl. Mater. Interfaces* **17**, 14016-14024 (2025).
28. Gao Y. *et al.* Steric-Hindrance-Engineered 1D/3D Heterojunction Unlocks Atomic-Level Matched Buried Interface for Efficient Perovskite Solar Cells. *ACS Appl. Mater. Interfaces* **17**, 39652-39662 (2025).